Applied Microscopy
Korean Society of Microscopy

pISSN 2287-5123 · eISSN 2287-4445
http://dx.doi.org/10.9729/AM.2012.42.3.174

Characterization of the Oxide Layer Formed on the Cu-Zr Based Metallic Glass during Continuous Heating

Ka Ram Lim, Won Tae Kim[1], Do Hyang Kim*

Center for Non-crystalline Materials, Department of Materials Science and Engineering, Yonsei University, Seoul 120-749, Korea
[1]Department of Optical Engineering, Cheongju University, Cheongju 360-764, Korea

*Correspondence to:
Kim DH,
Tel: +82-2-2123-4255
Fax: +82-2-312-8281
E-mail: dohkim@yonsei.ac.kr

Received September 6, 2012
Revised September 11, 2012
Accepted September 15, 2012

In the present study, the oxidation behavior of $Cu_{50}Zr_{50}$ and $Cu_{46}Zr_{46}Al_8$ metallic glasses has been investigated using transmission electron microscopy with a particular attention on the oxidation behavior in the supercooled liquid state. Identification of the oxidation product after continuous heating treatment shows that in $Cu_{50}Zr_{50}$ metallic glass, ZrO_2 with the monoclinic structure forms on the supercooled liquid as well as on the crystallized matrix. On the contrary, in $Cu_{46}Zr_{46}Al_8$ metallic glass, ZrO_2 with the tetragonal structure forms on the supercooled liquid, but that with the monoclinic structure forms on the crystallized matrix. The result indicates that the $Cu_{50}Zr_{50}$ metallic glass exhibits far better oxidation resistance in the supercooled liquid state than the $Cu_{46}Zr_{46}Al_8$ metallic glass.

Key Words: Oxidation, Supercooled liquid, Metallic glass, ZrO_2

INTRODUCTION

Recently, bulk metallic glasses (BMGs) have attracted increasing attention since they exhibit exotic properties which cannot be found in their counterpart crystalline alloys (Inoue, 2000). In particular, a lot of research activities are being performed for structural and functional applications of BMGs due to extremely high strength and hardness, large elastic strain limit combined with relatively high fracture toughness, as well as good wear and corrosion resistance (Corner et al., 1997; Gilbert et al., 1997; Park et al. 2002; Ma et al., 2004; Jayaraj et al., 2006). For structural application of BMGs, enhancement of the plasticity is one of the critical issues to be solved. Inherently, glassy alloys exhibit very high level of strength, but very low level of plasticity. There have been a lot of attempts to enhance the plasticity by providing a structural inhomogeneity in the glassy matrix, for example, it has recently been shown that a minor addition of an element that has positive enthalpy of mixing with some of the constituent elements is an effective way to improve the plasticity of BMGs by providing chemical and/or structural heterogeneity in the amorphous matrix (Xing et al., 2001; Lee et al., 2004; Oh et al., 2005; Park et al., 2005; Park et al., 2006; Park & Kim, 2006; Park et al., 2007). However, the level of the plasticity is still not enough to be applied as structural materials. On the contrary, there are several examples of successful application of BMGs as functional materials. One of the astonishing benefits of the BMGs is their excellent thermoplastic forming ability and wettability in the super-cooled liquid region. Using such advantages of BMGs, Kim et al. (2011) applied CuZr-based metallic glass as a binding agent of Ag paste for front contact formation in Si solar cell by screen printing process. They showed that use of electroconductive metallic glass binder significantly improves the quality of the contact by the formation of highly dense nm scale fine Ag crystallites and the noncorrugation of the emitter surface with a very shallow Ag crystallite penetration depth. Carmo et al. (2011) fabricated Pt-base metallic glass nanowires using a facile and scalable nanoimprinting approach to create dealloyed high surface area nanowire catalysts with high conductivity and activity

This work was supported by the Global Research Laboratory Program of the Korean Ministry of Education, Science and Technology.

for methanol and ethanol oxidation. They showed that these nanowires exhibit superior performance efficiency than the conventional Pt/C. Wang et al. (2012) reported that the MgZn-based metallic glass powders have excellent functional ability in degrading azo dyes which are typical organic water pollutants. Their azo dye degradation efficiency is about 1,000 times higher than that of commercial crystalline Fe powders, and 20 times higher than the Mg-Zn alloy crystalline counterparts. Moreover, they suggested that the high Zn content in the amorphous Mg-based alloy enables a greater corrosion resistance in water and higher reaction efficiency with azo dye compared to crystalline Mg.

Since most of the functional applications make use of high thermoplasticity and wettability of BMGs in the super-cooled liquid region, it is also highly required that BMGs should exhibit high oxidation resistance in the super-cooled liquid region. Most of the oxidation experiments on BMGs reported so far have been performed by exposing the BMG samples for long time at high temperature to evaluate the possibility for application as a structural material (Kimura et al., 1993; Tam & Shek, 2005; Tam & Shek, 2006; Köster et al., 2007; Kai et al., 2010). However, for functional application of BMGs the oxidation behavior and mechanism need to be examined in detail in the super-cooled liquid region for short time exposure.

Therefore, the aim of the present study is to investigate the oxidation resistance of Cu-Zr based metallic glasses during continuous heating up to the super-cooled liquid region. For fabrication in the super-cooled liquid state, one of the prime requirements is the selection of metallic glass which exhibits a wider temperature region of the super-cooled liquid region. Therefore, to increase the temperature region of the super-cooled liquid region, we have selected two alloy compositions of $Cu_{50}Zr_{50}$ and $Cu_{46}Zr_{46}Al_8$ (in at%). Since the temperature range of the super-cooled liquid region is closely related to the glass forming ability of the metallic glass (Inoue, 2000), we have selected Al as the third alloying element from the point of view of the enhancement of glass forming ability.

MATERIALS AND METHODS

Alloy ingots with the nominal compositions of $Cu_{50}Zr_{50}$ and $Cu_{46}Zr_{46}Al_8$ were produced by arc-melting high-purity metals with purities of 99.9% or higher under argon atmosphere in a water-cooled copper crucible. Rapidly solidified ribbons were prepared by remelting the alloys in quartz tubes and ejecting the melt with an overpressure of 50 kPa through a nozzle onto a copper wheel rotating with a surface velocity of 40 m/s.

The structure and the thermal stability of the melt-spun ribbon samples were examined using x-ray diffractometry (XRD; D8 DISCOVER; Bruker AXS, Billerica, MA, USA), differential scanning calorimetry (DSC 7; Perkin Elmer, Oxfordshire, UK), and differential thermal analysis (DTA 7; Perkin Elmer) at a heating rate of 40 K/min.

To characterize the oxide layer, the ribbon samples were continuously heated in thermogravimetric analyzer (TGA 4000; Perkin Elmer) in high-purity dry air (99.99%). Different heating temperatures were selected depending on the composition of the metallic glass. Characterization of the oxidation scales was performed using transmission electron microscopy (TEM; JEOL 2010F, Tokyo, Japan) equipped with an energy dispersive spectrometer (INCA x-act 51-ADD0069; Oxford Instruments, Waltham, MA, USA). To observe the full cross section of the oxide layer, the samples were prepared using a focused ion beam milling equipment (Dual-beam FIB; FEI Helios NanoLab, Hillsboro, OR, USA).

RESULTS AND DISCUSSION

The XRD results showed that the $Cu_{50}Zr_{50}$ and $Cu_{46}Zr_{46}Al_8$ melt-spun ribbon samples have a single amorphous structure. Thermal analysis revealed that the glass transition temperature (T_g) of the $Cu_{50}Zr_{50}$ and $Cu_{46}Zr_{46}Al_8$ samples are 685 K and 719 K, respectively and the crystallization onset temperature (T_x) are 738 K and 791 K, respectively. With the addition of Al in $Cu_{50}Zr_{50}$, the T_g increased by 34 K, but the T_x increased more significantly by 53 K, thereby the temperature region of the super-cooled liquid region (ΔT_x) increased from 53 K to 72 K. The result indicates that the glass forming ability of Cu-Zr based BMGs is improved with the addition of alloying element, Al.

Recent study (Lim et al., 2012) on the oxidation behavior of $Cu_{50}Zr_{50}$ and $Cu_{46}Zr_{46}Al_8$ metallic glasses after continuous heating up to 1073 K shows that for $Cu_{50}Zr_{50}$, the oxide layer mostly consists of monoclinic ZrO_2 (m-ZrO_2), while for $Cu_{46}Zr_{46}Al_8$, the oxide layer consists of two different layers: an outer layer consisting of tetragonal ZrO_2 (t-ZrO_2) + Al_2O_3 + metallic Cu (oxidation products from the super-cooled liquid state of the glass matrix) and inner layer comprised of m-ZrO_2 + metallic Cu islands (oxidation products from the crystallized matrix) (Lim et al., 2012). One of the important findings is that the addition of Al in $Cu_{50}Zr_{50}$ leads to a significant deterioration of the oxidation resistance in the super-cooled liquid state, although the glass forming ability is enhanced with the addition of Al. If Al is solutionized in ZrO_2, oxygen ion vacancy concentration increases, therefore, higher activity of oxygen ions can be provided. Under such a condition, the oxidation proceeds more actively, resulting in the deterioration of the oxidation resistance. Based on the previous report, the oxidation behavior in binary Cu-Zr metallic glass is compared with that of the ternary Cu-Zr-Al metallic glass in the present study by the detailed TEM study. Therefore, the two metallic glass samples were continuously heated up to different temperatures, i.e. for the $Cu_{50}Zr_{50}$

sample first up to 725 K (in the super-cooled liquid region) and then finally up to 1,073 K, and for the $Cu_{46}Zr_{46}Al_8$ sample first up to 673 K (below the T_g) and then finally up to 1,073 K. Fig. 1 shows the bright field (BF) TEM image obtained from the $Cu_{50}Zr_{50}$ sample continuously heated up to 725 K. The high resolution TEM image inserted in the BF TEM image clearly shows that the oxide layer is present in the crystalline state, while the matrix retains the glassy state. Since the sample was heated up to the temperature in the super-cooled liquid region, it is natural that the matrix remains in the glassy state as can be confirmed from the inserted Fast Fourier Transformed (FFT) diffraction pattern exhibiting a diffuse halo which is characteristic of the amorphous structure. The thickness of the oxide layer is ~15 nm, and is identified as m-ZrO_2 phase from the inserted FFT diffraction pattern exhibiting a [1-10] zone of the monoclinic structure. It is considered that the oxidation-protective m-ZrO_2 film which formed below the T_g suppresses the oxidation in the super-cooled liquid region.

Fig. 2 shows the BF TEM image obtained from the $Cu_{46}Zr_{46}Al_8$ sample continuously heated up to 673 K. Since the sample was heated below the glass transition temperature, the matrix remains in the glassy state as can be seen from the inserted selected area diffraction pattern (SADP). The thickness of the oxide layer is ~30 nm, and is identified as t-ZrO_2 phase from the inserted SADP exhibiting a [301] zone of the tetragonal structure.

Here, it has to be mentioned that there are three types of crystal structure for ZrO_2, i.e. monoclinic, tetragonal and cubic structures which can be differentiated according to the concentration of oxygen ion vacancies (Shukla & Seal, 2005). Among the three crystal structures, the monoclinic structure is most stable, thus has the highest oxidation resistance. On the contrary, the tetragonal structure is vulnerable to oxidation due to higher concentration of oxygen vacancies. Therefore, TEM observation results mentioned above indicate that binary $Cu_{50}Zr_{50}$ metallic glass exhibits better oxidation resistance than ternary $Cu_{46}Zr_{46}Al_8$ metallic glass, judging from the crystal structure of ZrO_2. As mentioned above, the addition of Al in Cu-Zr metallic glass increases the oxygen ion vacancy concentration, thus promoting the formation of t-ZrO_2. As a result, the oxidation resistance is deteriorated significantly.

Fig. 3 shows the BF TEM images obtained from the $Cu_{50}Zr_{50}$ and $Cu_{46}Zr_{46}Al_8$ samples continuously heated up to 1,073 K. Since the sample was heated up to the temperature above the crystallization onset temperature for both samples, the glassy matrix is crystallized after heating up to 1,073 K. The thickness of the oxide layer is ~1,200 nm and ~1,600 nm, respectively, again confirming that the ternary $Cu_{46}Zr_{46}Al_8$ metallic glass exhibits inferior oxidation resistance to the binary $Cu_{50}Zr_{50}$ metallic glass. From the XRD analysis result, the oxide scale of the $Cu_{50}Zr_{50}$ sample continuously heated up to 1,073 K consists mainly of ZrO_2 with the monoclinic structure, while the oxide scale of the $Cu_{46}Zr_{46}Al_8$ sample continuously heated up to 1,073 K consists of a mixture of ZrO_2 with the monoclinic and the tetragonal structure. Since ZrO_2 with the tetragonal structure forms in the supercooled liquid state (Fig. 2) of the $Cu_{46}Zr_{46}Al_8$ sample, it can be inferred that the oxide layer of ZrO_2 with the monoclinic structure forms on the crystallized $Cu_{46}Zr_{46}Al_8$ sample. Therefore, the oxide layer consists of two layers of inner and outer layer which are ZrO_2 with the monoclinic structure and ZrO_2 with the tetragonal structure, respectively, although it cannot be clearly differentiated in the BF TEM image (Fig.

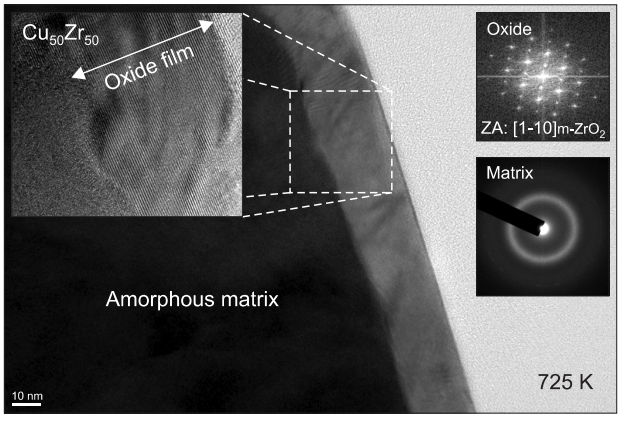

Fig. 1. Cross-sectional bright field (BF) transmission electron microscopy (TEM) image obtained from the $Cu_{50}Zr_{50}$ alloy showing the oxide thin-films after continuous heating up to 725 K (supercooled liquid region). The high resolution TEM image from the region marked in the BF TEM image is inserted. The Fast Fourier Transformed diffraction patterns obtained from the oxide layer and the matrix are also inserted.

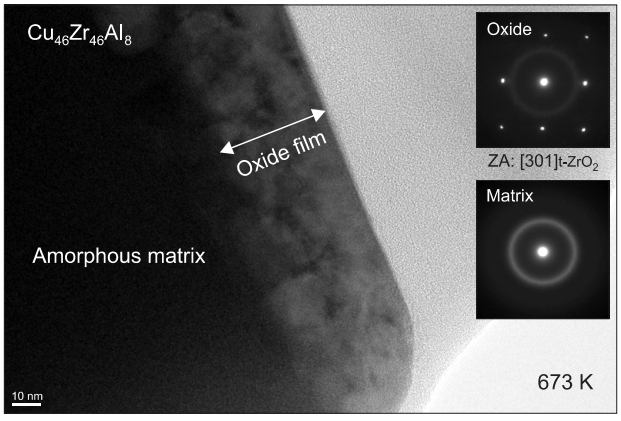

Fig. 2. Cross-sectional bright field transmission electron microscopy image obtained from the $Cu_{46}Zr_{46}Al_8$ alloy showing the oxide thin-films after continuous heating up to 673 K (below the glass transition temperature). The selected area diffraction patterns obtained from the oxide layer and the matrix are inserted.

3B). On the contrary, in the case of $Cu_{50}Zr_{50}$ metallic glass sample, the oxide layer of ZrO_2 with the monoclinic structure forms on the crystallized matrix as well as on supercooled liquid matrix, resulting in superior oxidation resistance. To confirm the formation of ZrO_2 with the monoclinic structure on the crystallized $Cu_{46}Zr_{46}Al_8$ sample, additional experiment was performed: the $Cu_{46}Zr_{46}Al_8$ metallic glass sample was heated above the T_g in an inert atmosphere to induce the crystallization of the glassy sample, and then the crystallized sample was heated from room temperature up to 1,073 K in an air atmosphere to identify the oxide layer which formed on the crystallized matrix. The XRD result shown in Fig. 4 indicates that ZrO_2 with the monoclinic structure is the main oxidation product which grows on the crystallized $Cu_{46}Zr_{46}Al_8$ sample. The result clearly confirms that the oxide which forms on the supercooled liquid of the $Cu_{46}Zr_{46}Al_8$ sample is ZrO_2 with the tetragonal structure, while that formed on the crystallized $Cu_{46}Zr_{46}Al_8$ sample is ZrO_2 with the monoclinic structure.

In general, it is known that the oxidation resistance of the amorphous alloys is linked to their ability to form amorphous oxide since the grain boundaries which provide a rapid diffusion path is absent in the amorphous oxide (Scully & Lucente, 2005). The interface between the amorphous oxide and the amorphous alloy matrix can have a lower energy due to enhanced bond flexibility. In other words, the lattice mismatch and strain can be easily relieved at the interface due to rather easy rearrangement of atoms or ions in the amorphous structure. However, the formation of the amorphous oxide was not observed in the present study. When considering that the thickness of the initial amorphous oxide layer which forms on the pure metal is only a few nm, a thin amorphous oxide layer may form on the glassy matrix at the very early stage of oxidation. Such amorphous oxide layer transforms into different crystalline oxide layer, depending the alloy chemistry of the glassy matrix. Considering the oxidation resistance of metallic glass in the super-cooled liquid state, it is very important that what kind of oxide film is formed on the surface of the metallic glass in the supercooled liquid region. In this study, the $Cu_{50}Zr_{50}$ metallic glass forms ZrO_2 film with the monoclinic structure (protective in the supercooled liquid region), while the $Cu_{46}Zr_{46}Al_8$ metallic glass has ZrO_2 film with the tetragonal structure (non-protective in the supercooled liquid region).

CONCLUSIONS

In the present study, the oxidation behavior of $Cu_{50}Zr_{50}$ and $Cu_{46}Zr_{46}Al_8$ metallic glasses has been investigated using TEM with a prime concern on the oxidation behavior in the supercooled liquid state. In $Cu_{50}Zr_{50}$ metallic glass, ZrO_2 with the monoclinic structure forms on the supercooled liquid as well as on the crystallized matrix. On the contrary, in $Cu_{46}Zr_{46}Al_8$ metallic glass, ZrO_2 with the tetragonal structure forms on the supercooled liquid, but that with the monoclinic structure forms on the crystallized matrix. Considering that the oxygen vacancy is more abundant in the tetragonal structure than in the monoclinic structure of ZrO_2, the $Cu_{50}Zr_{50}$ metallic glass exhibits far better oxidation resistance in the supercooled liquid state than the $Cu_{46}Zr_{46}Al_8$ metallic glass.

ACKNOWLEDGMENTS

K. R. Lim acknowledges the support from the Second Stage of Brain Korea 21 Project.

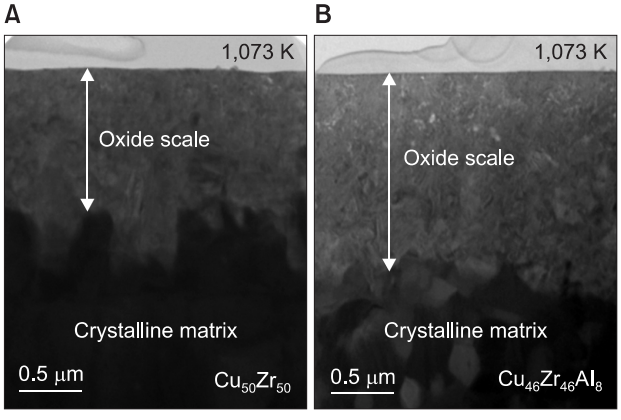

Fig. 3. Cross-sectional bright field transmission electron microscopy images obtained from: (A) the $Cu_{50}Zr_{50}$ alloy; and (B) the $Cu_{46}Zr_{46}Al_8$ alloy showing the oxide thin-films after continuous heating up to 1,073 K.

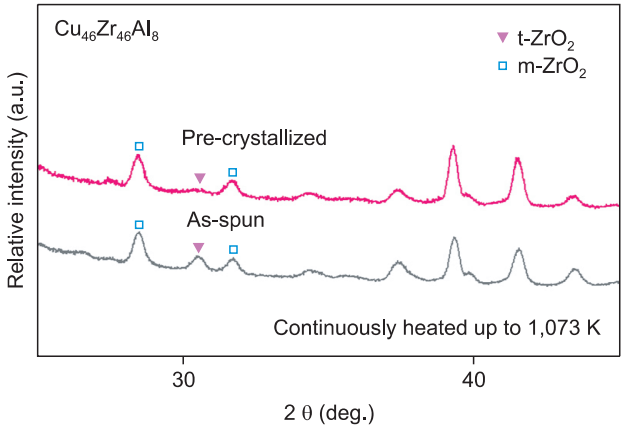

Fig. 4. The x-ray diffractometry pattern obtained from the $Cu_{46}Zr_{46}Al_8$ alloy heated above the crystallization onset temperature. The crystallized sample was continuously heated up to 1,073 K.

REFERENCES

Carmo M, Sekol R C, Ding S Y, Kumar G, Schroers J, and Taylor A D (2011) Bulk metallic glass nanowire architecture for electrochemical applications. *ACS Nano* **5**, 2979-2983.

Conner R D, Rosakis A J, Johnson W L, and Owen D M (1997) Fracture toughness determination for a beryllium-bearing bulk metallic glass. *Scripta. Mater.* **37**, 1373-1378.

Gilbert C J, Ritchie R O, and Johnson W L (1997) Fracture toughness and fatigue-crack propagation in a Zr-Ti-Ni-Cu-Be bulk metallic glass. *Appl. Phys. Lett.* **71**, 476-478.

Inoue A (2000) Stabilization of metallic supercooled liquid and bulk amorphous alloys. *Acta. Mater.* **48**, 279-306.

Jayaraj J, Sordelet D J, Kim D H, Kim Y C, and Fleury E (2006) Corrosion behavior of Ni-Zr-Ti-Si-Sn amorphous plasma spray coating. *Corros. Sci.* **48**, 950-964.

Kai W, Kao P C, Lin P C, Ren I F, and Jang J S C (2010) Effects of Si addition on the oxidation behavior of a Cu–Zr-based bulk metallic alloy. *Intermetallics* **18**, 1994-1999.

Kim S Y, Jee S S, Lim K R, Kim W T, Kim D H, Lee E S, Kim T H, Lee S M, Lee J H, and Eckert J (2011) Replacement of oxide glass with metallic glass for Ag screen printing metallization on Si emitter. *Appl. Phy. Lett.* **98**, 222112.

Kimura H M, Asami K, Inoue A, and Masumoto T (1993) The oxidation of amorphous Zr-based binary alloys in air. *Corros. Sci.* **35**, 909-915.

Köster U, Jastrow L, and Meuris M (2007) Oxidation of Cu60Zr30Ti10 metallic glasses. *Mater. Sci. Eng. A* **449**, 165-168.

Lee M H, Lee J Y, Bae D H, Kim W T, Sordelet D J, and Kim D H (2004) A development of Ni-based alloys with enhanced plasticity. *Intermetallics* **12**, 1133-1137.

Lim K R, Kim W T, Lee E S, Jee S S, Kim S Y, Kim D H, Gebert A, and Eckert J (2012) Oxidation resistance of the supercooled liquid in Cu50Zr50 and Cu46Zr46Al8 metallic glasses. *J. Mater. Res.* **27**, 1178-1186.

Ma M Z, Liu R P, Xiao Y, Lou D C, Liu L, Wang Q, and Wang W K (2004) Wear resistance of Zr-based bulk metallic glass applied in bearing rollers. *Mater. Sci. Eng. A* **386**, 326-330.

Oh J C, Ohkubo T, Kim Y C, Fleury E, and Hono K (2005) Phase separation in Cu43Zr43Al7Ag7 bulk metallic glass. *Scripta. Mater.* **53**, 165-169.

Park E S, Chang H J, Kim D H, Ohkubo T, and Hono K (2006) Effect of substitution of Ag and Ni for Cu on the glass forming ability and plasticity of Cu60Zr30Ti10 alloy. *Scripta. Mater.* **54**, 1569-1573.

Park E S and Kim D H (2006) Phase separation and enhancement of plasticity in Cu-Zr-Al-Y bulk metallic glass. *Acta. Mater.* **54**, 2597-2604.

Park E S, Kim D H, Ohkubo T, and Hono K (2005) Enhancement of glass forming ability and plasticity by addition of Nb in Cu-Ti-Zr-Ni-Si bulk metallic glass. *J. Non-Cryst. Solids.* **351**, 1232-1238.

Park E S, Kyeong J S, and Kim D H (2007) Phase separation and improved plasticity by modulated heterogeneity in Cu-(Zr, Hf)-(Gd, Y)-Al metallic glasses. *Scripta. Mater.* **57**, 49-52.

Park E S, Lim H K, Kim W D, Kim D H (2002) The effect of Sn addition on the glass-forming ability of Cu-Ti-Zr-Ni-Si metallic glass alloys. *J. Non-Crys. Solids.* **298**, 15-22.

Scully J R and Lucente A (2005) Corrosion of amorphous metals. In: *ASM Handbook, Volume 13B: Corrosion: Materials*, ed. Cramer S D and Covino B S, pp. 476-489, (ASM International, Russell Township, Geauga County).

Shukla S and Seal S (2005) Mechanisms of room temperature metastable tetragonal phase stabilization in zirconia. *Int. Mater. Rev.* **50**, 45-64.

Tam C Y and Shek C H (2005) Oxidation behavior of Cu60Zr30Ti10 bulk metallic glass. *J. Mater. Res.* **20**, 1396-1403.

Tam C Y and Shek C H (2006) Oxidation-induced copper segregation in Cu60Zr30Ti10 bulk metallic glass. *J. Mater. Res.* **21**, 851-855.

Wang J Q, Liu Y H, Chen M W, Louzguine-Luzgin D V, Inoue A, and Perepezko J H (2012) Excellent capability in degrading azo dyes by MgZn-based metallic glass powders. *Scientific Reports* **2**, 418.

Xing L-Q, Li Y, Ramesh K T, Li J and Hufnagel T C (2001) Enhanced plastic strain in Zr-based bulk amorphous alloys. *Phys. Rev. B* **64**, 180201(R).